A Study of Synchronization in Chaotic Autonomous Ćuk DC/DC Converters

H. H. C. Iu and C. K. Tse

***Abstract*—The synchronization property of chaotic free-running dc/dc converters is studied in this paper. The system under study consists of two Ćuk converters operating under free-running current-mode control, with two converters connected in the well-known drive-response configuration similar to that studied by Pecora and Carroll. This paper studies, in particular, the synchronization property of the system when a capacitor voltage is chosen as the driving signal. The study includes the derivation of the describing differential equations and the calculation of the conditional Lyapunov exponents (CLE's) of the synchronizing system based on the differential equations. It is found that all the CLE's are negative for certain chosen parameters and, hence, synchronization is possible in this system. Exact computer simulations have been performed to verify the synchronization of the aforedescribed circuits operating in chaotic regime. With the drive-response system connected, synchronization is demonstrated using both exact time-domain simulations and PSPICE simulations. This paper reports for the first time the synchronization phenomenon in power electronic converters.**

***Index Terms*—Chaos synchronization, coupled chaotic circuits, power electronics, switching converters.**

I. Introduction

Since Pecora and Carroll [1], [2] demonstrated the possibility of synchronizing two chaotic systems, many investigations have been carried out to explore the properties and applications of chaos synchronization in a range of nonlinear circuits and systems [3]–[7]. For power electronics systems, although chaos and bifurcation have been identified in a number of practical converter configurations, e.g., dc/dc converters [8]–[13], not much has been reported on the possibility of chaos synchronization. Furthermore, recent success in applying chaos to communications may suggest possible use of chaotic power converters for such applications. If power converters could be used to transmit messages, then we may speculate, however immature at this stage, that future distributed power systems may be designed to serve the dual function of a power supply system and a medium of communication. Of course, a prerequisite is a well-informed operation of power converters in chaotic regimes for which further investigation is still needed.

In this paper, we consider a very common converter circuit, namely, the Ćuk converter and, in particular, its synchronization property when operating chaotically under a very simple free-running current-programmed scheme [14], [15]. The circuit configured as such can be modeled as an autonomous third-order system. Our purpose in this paper is to show that two such autonomous systems, connected in a drive-response configuration similar to that considered by Pecora and Carroll [1], [2] can be synchronized. We will first show mathematically and numerically that the conditional Lyapunov exponents (CLE's) of the coupled system under study are negative, and, hence, synchronization is possible. Finally, computer simulations of the actual system confirm the predicted synchronization phenomenon.

Manuscript received December 24, 1998; revised September 16, 1999. This work is supported by in part by a competitive earmarked research grant from the Hong Kong Research Grants Council. This paper was recommended by Associate Editor C. W. Wu.

The authors are with the Department of Electronic and Information Engineering, The Hong Kong Polytechnic University, Kowloon, Hong Kong, China.

Publisher Item Identifier S 1057-7122(00)05050-9.

II. Review of Drive-Response Configuration

One essential property of a chaotic system is that trajectories starting from nearby initial conditions diverge exponentially with time and quickly become uncorrelated. It is therefore nontrivial to show that two chaotic systems coupled through a chaotic signal can be in perfect synchronization. In Pecora and Carroll [1], [2] such a possibility was demonstrated. The basic idea of Pecora and Carroll can be briefly described as follows.

Consider an n-dimensional $(n = m + k)$ dynamical system which is described by a state equation of the form

$$\dot{\overline{x}} = f(\overline{x}(t)) \tag{1}$$

where $\overline{x} = [x_1 \ x_2 \ \cdots \ x_n]^T$. The system is divided into two subsystems in an arbitrary way. Accordingly, the state vector $\overline{x}$ is partitioned as $\overline{x} = [\overline{x}_D \ \overline{x}_R]^T$, where $\overline{x}_D$ is an m-dim vector and $\overline{x}_R$ is a k-dim vector corresponding to a drive subsystem and a response subsystem, respectively, i.e., $\overline{x}_D = [x_1 \ x_2 \ \cdots \ x_m]^T$ and $\overline{x}_R = [x_{m+1} \ x_{m+2} \ \cdots \ x_n]^T$. Then, (1) can be rewritten as

$$\begin{aligned} \dot{\overline{x}}_D &= g(\overline{x}_D, \overline{x}_R) \\ \dot{\overline{x}}_R &= h(\overline{x}_D, \overline{x}_R) \end{aligned} \tag{2}$$

where $g(\overline{x}) = [f_1(\overline{x}) \cdots f_m(\overline{x})]^T$ and $h(\overline{x}) = [f_{m+1}(\overline{x}) \cdots f_n(\overline{x})]^T$.

An identical copy of the system is constructed and driven by $\overline{x}_D$ taken from the above original system. We let the state variables of this new system be $\overline{x}'$ which is likewise partitioned, i.e., $\overline{x}' = [\overline{x}'_D \ \overline{x}'_R]^T$. The dynamics of this second system is thus described by

$$\begin{aligned} \dot{\overline{x}}'_D &= g(\overline{x}_D, \overline{x}'_R) \\ \dot{\overline{x}}'_R &= h(\overline{x}_D, \overline{x}'_R). \end{aligned} \tag{3}$$

Since $\overline{x}'_D = \overline{x}_D$, we may ignore the dynamics of $\overline{x}'_D$ and, hence, describe the second system by only its response subsystem equation, i.e.,

$$\dot{\overline{x}}'_R = h(\overline{x}_D, \overline{x}'_R). \tag{4}$$

Now, the original system (2) and the second response subsystem (4) constitute a complete coupled system.

It is readily shown that if all the Lyapunov exponents of the second response subsystem (4), also called conditional Lyapunov exponents (CLE's), are negative, then after the decay of the initial transient, $\overline{x}'_R$ will be exactly in step with $\overline{x}_R$. More precisely, under perfect synchronization the difference between $\overline{x}'_R$ and $\overline{x}_R$ will tend to zero asymptotically, i.e., $\lim_{t\to\infty} |\overline{x}'_R - \overline{x}_R| = 0$. Alternatively, one may examine the error system that describes the dynamics of $(\overline{x}'_R - \overline{x}_R)$. Letting $\overline{e}_R$ be $(\overline{x}'_R - \overline{x}_R)$, we can write $\dot{\overline{e}}_R(t) = h(\overline{x}_D, \overline{x}'_R) - h(\overline{x}_D, \overline{x}_R)$, or

$$\dot{\overline{e}}_R(t) = h_e(\overline{x}_D, \overline{x}_R, \overline{x}'_R). \tag{5}$$

The Lyapunov exponents of this system are also the CLE's. If h_e is linear, we can examine its eigenvalues and conclude that synchronization occurs if the real parts of all these eigenvalues are negative. Note that the real parts of these eigenvalues are also the CLE's. When h_e is nonlinear, we must resort to numerical procedure in order to calculate the CLE's.

For brevity, we will refer to the original system as the drive system (with state vector $\overline{x}$)and to the second system as the response system (with state vector $\overline{x}'$).

1057–7122/00$10.00 © 2000 IEEE

Authorized licensed use limited to: Hong Kong Polytechnic University. Downloaded on December 18, 2008 at 21:24 from IEEE Xplore. Restrictions apply.

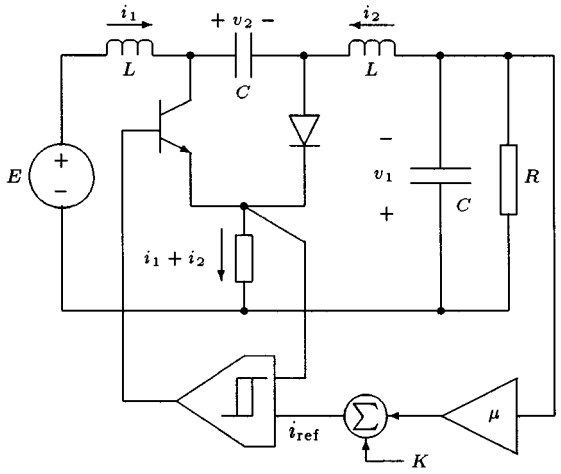

Fig. 1. Ćuk converter under hysteretic current-mode control.

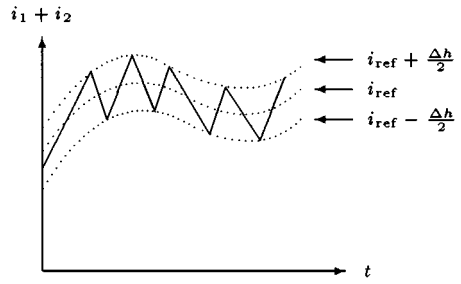

Fig. 2. Hysteretic current-programming scheme.

III. Free-Running Current-Programmed Ćuk Converter

A. Piecewise Switched Model

The free-running current-programmed Ćuk converter under study is shown in Fig. 1 [14], [15]. The circuit operation can be described as follows. The sum of the inductance currents, i.e., $i_1 + i_2$, is compared with a reference current $i_{\rm ref}$ in a hysteretic fashion. When $i_1 + i_2$ rises above $i_{\rm ref} + (\Delta h/2)$, where Δh is the width of a hysteretic band, the switch is turned off. When $i_1 + i_2$ falls below $i_{\rm ref} - (\Delta h/2)$, the switch is turned on. The reference current $i_{\rm ref}$ is related to the output voltage v_1 by a feedback equation

$$i_{\rm ref} = K - \mu v_1 \tag{6}$$

where K and μ are the control parameters. Fig. 2 illustrates this current-programming scheme.

The converter itself can be represented by the following set of state-space equations, where $s = 1$ when the switch is closed, and $s = 0$ when the switch is open

$$\begin{aligned}
\frac{di_1}{dt} &= -\frac{(1-s)v_2}{L} + \frac{E}{L} \\
\frac{di_2}{dt} &= \frac{v_2 s}{L} - \frac{v_1}{L} \\
\frac{dv_1}{dt} &= \frac{i_2}{C} - \frac{v_1}{CR} \\
\frac{dv_2}{dt} &= \frac{(1-s)i_1}{C} - \frac{i_2 s}{C}.
\end{aligned} \tag{7}$$

The above equations constitute an exact piecewise switched model for the Ćuk converter, which will be used for computer simulations of the actual system to be reported in a later section.

B. State-Space Averaged Model

The state-space averaging approach has been widely used for modeling dc/dc converters [16]. For the Ćuk converter, the state-space averaged model has the same form as (7), with s replaced by the duty cycle δ which is the fraction of the switching period for which the switch is closed. From (6), we see that the current-programming scheme essentially forces $i_1 + i_2$ to be linearly related to v_2 and if Δh is sufficiently small, we can write

$$i_1 + i_2 = K - \mu v_1. \tag{8}$$

The closed-loop system is thus reduced to third order and the state-space averaged model becomes

$$\begin{aligned}
\frac{di_2}{dt} &= \frac{v_2\delta}{L} - \frac{v_1}{L} \\
\frac{dv_1}{dt} &= \frac{i_2}{C} - \frac{v_1}{CR} \\
\frac{dv_2}{dt} &= \frac{(1-\delta)(K-\mu v_1)}{C} - \frac{i_2}{C}
\end{aligned} \tag{9}$$

where δ is the duty cycle. From (8), we get $d(i_1 + i_2)/dt = -\mu\, dv_1/dt$. Substitution of the involving derivatives gives

$$\delta = \frac{1}{2} - \frac{\dfrac{\mu L}{C} i_2 - \left(1 + \dfrac{\mu L}{CR}\right) v_1 + E}{2v_2} \tag{10}$$

which must satisfy $0 < \delta < 1$. Finally, putting (10) into (9) results in the following set of autonomous state equations that describes the dynamics of the free-running current-programmed Ćuk converter:

$$\begin{aligned}
\frac{di_2}{dt} &= -\frac{\mu i_2}{2C} - \left(1 - \frac{\mu L}{CR}\right)\frac{v_1}{2L} + \frac{v_2}{2L} - \frac{E}{2L} \\
\frac{dv_1}{dt} &= \frac{i_2}{C} - \frac{v_1}{CR} \\
\frac{dv_2}{dt} &= -\frac{i_2}{C} + \left(\frac{K-\mu v_1}{2C}\right) \\
&\quad \cdot \left(1 + \frac{\dfrac{\mu L}{C} i_2 - \left(1 + \dfrac{\mu L}{CR}\right) v_1 + E}{v_2}\right).
\end{aligned} \tag{11}$$

Remarks: The above representation is valid only when there is no saturation of the duty cycle δ of the converter, i.e., $0 < \delta < 1$. However, in the real system saturation does occur, especially when it is operating in chaotic regime. Thus, when we use (11) to calculate the corresponding CLE's, we must take into account the saturation of the duty cycle δ.

C. Dimensionless Equation

Equation (11) can be put in a dimensionless form for the sake of simplicity. Define the dimensionless state variables as follows:

$$x_1 = \frac{Ri_2}{E}, \quad x_2 = \frac{v_1}{E}, \quad x_3 = \frac{v_2}{E}. \tag{12}$$

Also define the dimensionless time and other parameters as follows:

$$\tau = \frac{Rt}{2L}, \quad \xi = \frac{L/R}{CR}, \quad \kappa_1 = \mu R, \quad \kappa_0 = \frac{KR}{E}. \tag{13}$$

Direct substitution of these new dimensionless variables, time and parameters in the autonomous equation (11) gives the following dimensionless autonomous equations:

$$\begin{aligned}
\frac{dx_1}{d\tau} &= -\xi\kappa_1 x_1 - (1 - \kappa_1\xi)x_2 + x_3 - 1 \\
\frac{dx_2}{d\tau} &= 2\xi(x_1 - x_2) \\
\frac{dx_3}{d\tau} &= -2\xi x_1 + \xi(\kappa_0 - \kappa_1 x_2) \\
&\quad \cdot \left(1 + \frac{\kappa_1\xi x_1 - (1 + \kappa_1\xi)x_2 + 1}{x_3}\right).
\end{aligned} \tag{14}$$

Authorized licensed use limited to: Hong Kong Polytechnic University. Downloaded on December 18, 2008 at 21:24 from IEEE Xplore. Restrictions apply.

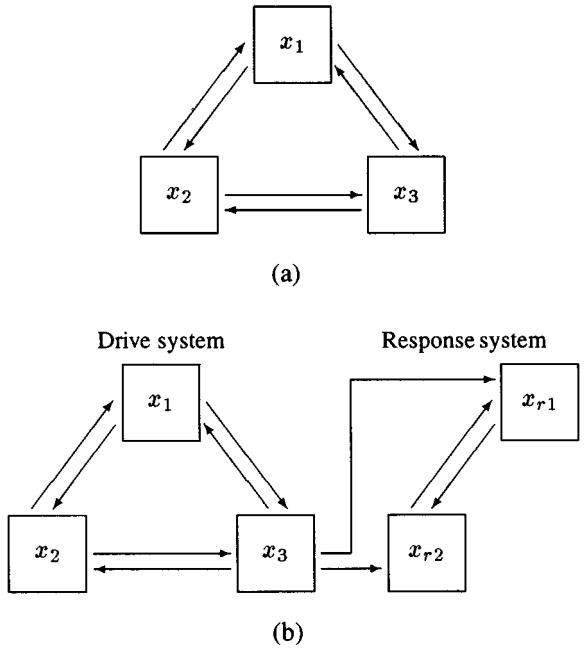

Fig. 3. Interaction of state variables in (a) isolated converter and (b) coupled converters in drive-response configuration.

In the next section, we will use this set of dimensionless equations to predict the synchronization property of chaotic Ćuk converters under free-running current-mode control.

IV. Chaos Synchronization in Free-Running Current-Programmed Ćuk Converters

A. Construction of Drive-Response System

We consider now two identical Ćuk converters arranged in the drive-response configuration described in Section II. Let x_1, x_2 and x_3 be the state variables of the drive converter, and x_{1r}, x_{2r} and x_{3r} be those of the response converter. In particular, we use x_3, i.e., the dimensionless equivalence of capacitor voltage v_2, as the driving signal.

The fifth-order coupled system is thus completely described by the set of drive converter equations, i.e., (14), and the set of response converter equations which is

$$\begin{aligned}\frac{dx_{r1}}{d\tau} &= -\xi\kappa_1 x_{r1} - (1-\kappa_1\xi)x_{r2} + x_3 - 1\\ \frac{dx_{r2}}{d\tau} &= 2\xi(x_{r1} - x_{r2})\end{aligned} \tag{15}$$

where subscript r denotes the response system variables. Fig. 3(a) describes the interaction of the variables for the case of the isolated converter, and Fig. 3(b) describes that for the case of the two converters being connected in the drive-response configuration.

B. Derivation of the Conditional Lyapunov Exponents

As mentioned in Section II, synchronization may be examined in terms of the error system, i.e., (5). For the system under study, the error system is linear. Letting $e_1 = x_1 - x_{r1}$ and $e_2 = x_2 - x_{r2}$, we can describe the error dynamics by

$$\begin{bmatrix}\dfrac{de_1}{d\tau}\\ \dfrac{de_2}{d\tau}\end{bmatrix} = \begin{bmatrix}-\xi\kappa_1 & -(1-\kappa_1\xi)\\ 2\xi & -2\xi\end{bmatrix}\begin{bmatrix}e_1\\ e_2\end{bmatrix}. \tag{16}$$

For brevity, we let $e = [e_1\ e_2]^T$ and put (16) as

$$\dot{e}(\tau) = Ae(\tau) \tag{17}$$

TABLE I
Comparison of CLEs from Averaged Model and by Numerical Calculation Incorporating Duty Cycle Saturation

κ_1	$\Re(\lambda_i)$ from (18)	$\Re(\lambda_i)$ from numerical calculation
0.5	−0.125	−0.12
1.0	−0.15	−0.13
1.5	−0.175	−0.15
2.0	−0.20	−0.17

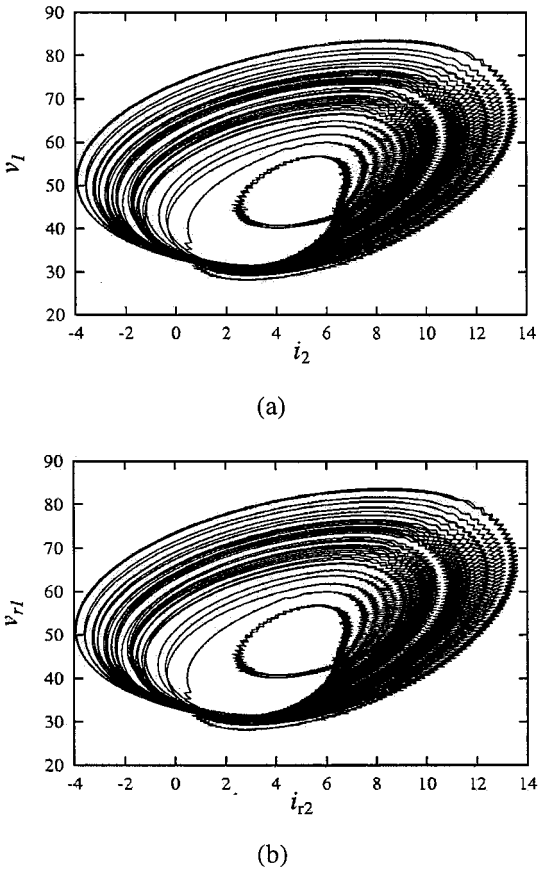

Fig. 4. Chaotic trajectory from exact time-domain simulation of (a) drive system and (b) response system.

where A can be extracted from (16). Our objective is to find the CLE's in order to determine if synchronization is possible. As mentioned in Section II, the real parts of the eigenvalues of the error system are in fact the CLE's we need to find. Let λ_1 and λ_2 be the eigenvalues of A. For this linear system, we can readily show that

$$\lambda_{1,2} = -\frac{(2\xi + \kappa_1\xi) \pm \sqrt{(2\xi+\kappa_1\xi)^2 - 8\xi}}{2}. \tag{18}$$

Clearly, for $(2\xi + \kappa_1\xi)^2 \geq 8\xi$, both eignevalues are negative. For $(2\xi + \kappa_1\xi)^2 < 8\xi$, moreover, the real part of both eigenvalues is negative for all positive values of κ_1 and ξ, i.e.,

$$\Re(\lambda_i) < 0 \quad \text{for all } \xi, \kappa_1 > 0. \tag{19}$$

Thus, by choosing suitable values of ξ, κ_1 and κ_0, the drive system can be set to operate in the chaotic regime (characterized by one positive Lyapunov exponent) and the response system will also be driven to chaos when synchronization occurs.

Authorized licensed use limited to: Hong Kong Polytechnic University. Downloaded on December 18, 2008 at 21:24 from IEEE Xplore. Restrictions apply.

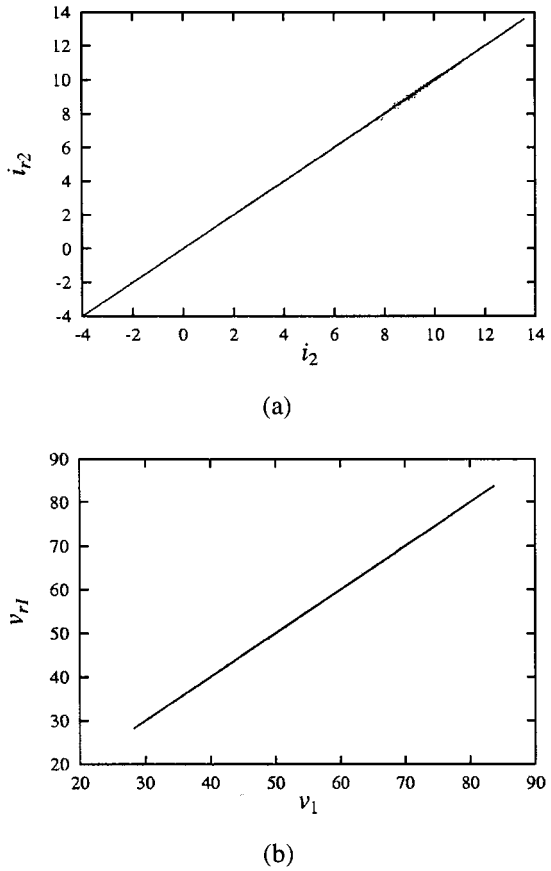

Fig. 5. Graphical representation of synchronization from exact time-domain simulation. (a) i_{r2} versus i_2. (b) v_{r1} versus v_1.

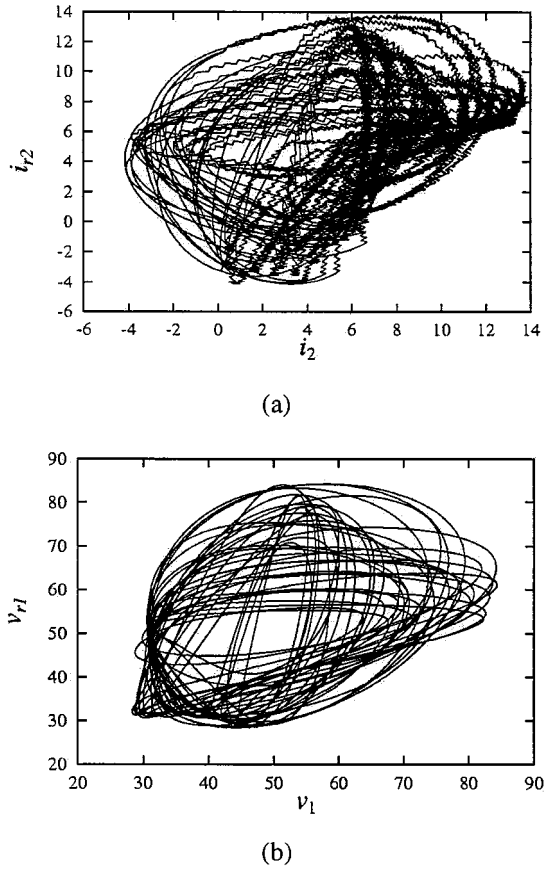

Fig. 6. Plots of (a) i_{r2} versus i_2 and (b) v_{r1} versus v_1 for the uncoupled converters.

C. Numerical Calculation of the Conditional Lyapunov Exponents

In the foregoing subsection, we have predicted that chaos synchronization is possible in the autonomous Ćuk converter. However, since the foregoing analysis is based on an averaged model of the converter which does not take into account the saturation of the duty cycle, the values of CLE's so obtained, i.e., those from (18), remain to be verified.

In this subsection, we will recalculate the CLE's numerically, taking into account the saturation effect. In other words, we will consider the realistic case in which the switch can remain in the ON (or OFF) state continuously, as a result of the action of the control scheme. Specifically, the describing equation for $\delta = 1$ is

$$\begin{aligned} \frac{dx_1}{d\tau} &= 2(x_3 - x_2) \\ \frac{dx_2}{d\tau} &= 2\xi(x_1 - x_2) \\ \frac{dx_3}{d\tau} &= -2\xi x_1 \end{aligned} \tag{20}$$

and that for $\delta = 0$ is

$$\begin{aligned} \frac{dx_1}{d\tau} &= -2x_2 \\ \frac{dx_2}{d\tau} &= 2\xi(x_1 - x_2) \\ \frac{dx_3}{d\tau} &= -2\xi x_1 + 2\xi(\kappa_0 - \kappa_1 x_2). \end{aligned} \tag{21}$$

Essentially we need to include two extra subroutines to generate the flow according to (20) and (21), when the calculated duty cycle exceeds one and falls below zero, respectively.

Actual numerical calculation has been performed by using the INSITE software[1] [17], which employs a Gram–Schmidt orthonormalization procedure for calculating Lyapunov exponents. In particular, we fix ξ at 0.1 which corresponds to a realistic practical choice, and for a range of κ_1 we have numerically calculated the corresponding CLE's using INSITE. The results are compared to those obtained from (18). As shown in Table I, the numerical CLE's are all negative and reasonably close to those obtained from (18). We may thus conclude that chaos synchronization is possible in the free-running current-programmed Ćuk converter under study. Verification is yet to be sought using computer simulation of the actual converter circuits.

Remarks: Up to this point, validity of the averaged model has been assumed. However, as studied in [15], averaged models are only good up to the point of losing stability. Thus, as long as synchronization is maintained, the averaged model for the error system is still valid and, in this case, synchronization should be predicted by the averaged model. The converse is not true, however, and one cannot draw any definite conclusion if the averaged model predicts failure of synchronization.

V. Computer Simulations

A. Exact Time-Domain Simulations for Piecewise Switched Model

In this section, we present exact simulations of the system under study, which consists of two identical free-running current-programmed Ćuk converters connected in the drive-response configuration, as described previously. Specifically, the drive system

[1]INSITE is a collection of software programs developed by T. S. Parker for studying chaotic systems. The particular software components used in this paper are LYEXP and TRAJ for generating Lyapunov exponents and trajectories.

Authorized licensed use limited to: Hong Kong Polytechnic University. Downloaded on December 18, 2008 at 21:24 from IEEE Xplore. Restrictions apply.

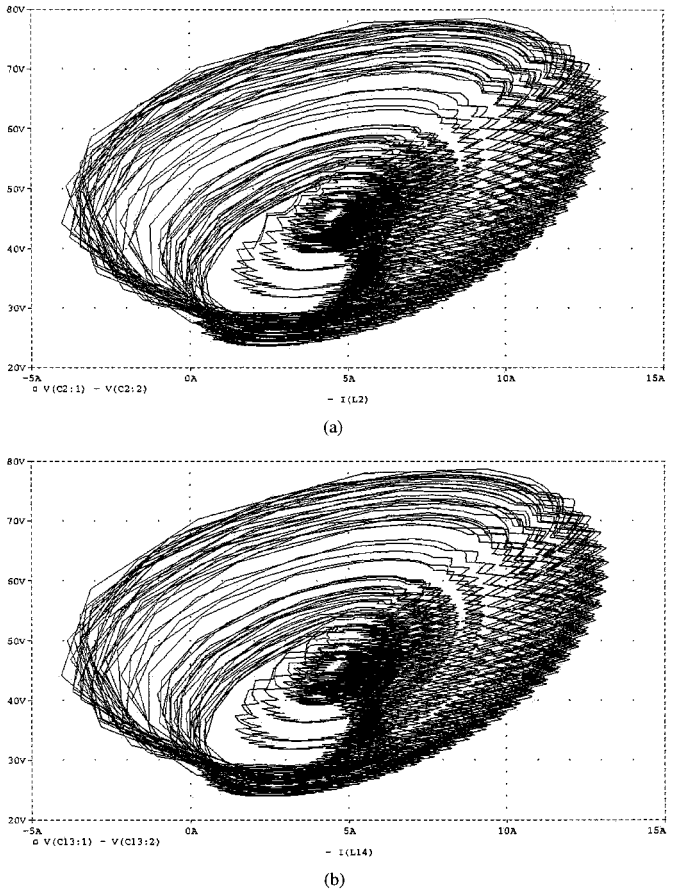

Fig. 7. Chaotic trajectory from PSPICE simulation of (a) drive system and (b) response system.

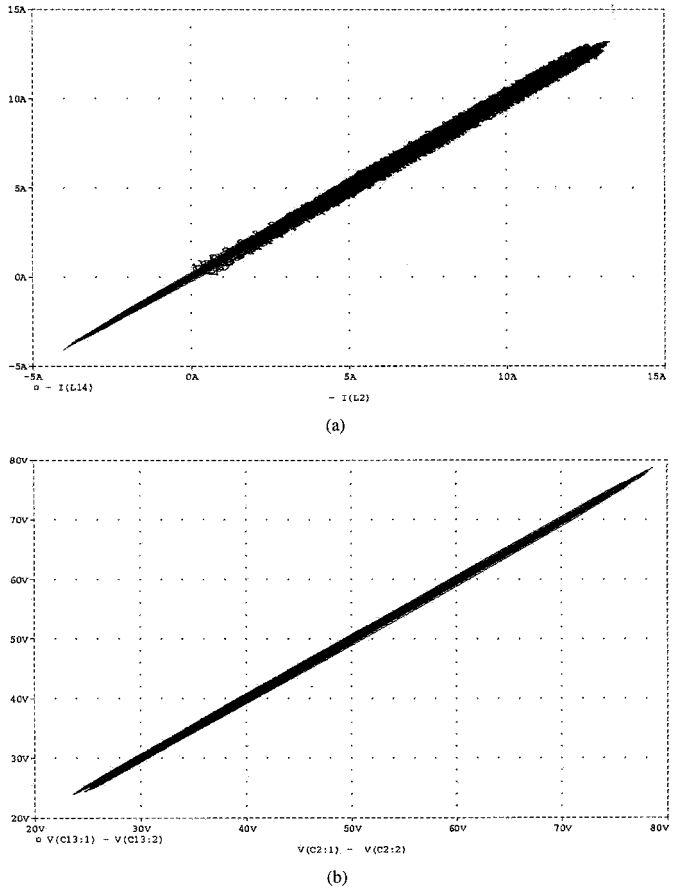

Fig. 8. Graphical representation of synchronization from PSPICE simulation. (a) i_{r2} versus i_2 and v_{r1} versus v_1.

is exactly the circuit shown in Fig. 1, and the response system is constructed with the middle capacitor (the one connecting the two inductors) replaced by a voltage-controlled voltage source which copies the value of v_2 from the drive system.

Based on the piecewise switched model developed in Section III-A, we have simulated the cycle-by-cycle waveforms of the actual circuit, from which the phase portraits of the drive and response systems are obtained. The values of the parameters used are $L = 0.01$ H, $C = 1000$ μF, $R = 10\ \Omega$, $E = 12$ V, $\Delta h = 0.5$ A, $\mu = 0.2$, and $K = 40$. These values correspond to $\xi = 0.1$, $\kappa_1 = 2.0$, and $\kappa_0 = 33.3$.

For ease of reporting, we use i_1, i_2, v_1, and v_2 to denote variables of the drive circuit, consistent with Fig. 1, and i_{1r}, i_{2r}, v_{1r}, and v_{2r} to denote those of the response circuit. The following results are presented.

1. Fig. 4 shows the chaotic trajectories of the drive system and the response system after discarding the points in the transient period.
2. Fig. 5 shows the curves of i_2 versus i_{r2}, and of v_1 versus v_{r1}, which verify that chaos synchronization is achieved.
3. For comparison, we have simulated the uncoupled system. The result is shown in Fig. 6.

B. PSPICE Simulations

The above simulations have verified the possibility of chaos synchronization in the theoretical circuit consisting of ideal switches and zero-delay switching. For further verification, we consider real MOSFET switches and practical gate drivers, and use PSPICE to simulate the system. Moreover, a voltage-controlled voltage source is again used to establish the coupling connection. The parameters used here are identical to those used in Section V-A. The results are shown in Figs. 7 and 8, which are in perfect agreement with those obtained in Section V-A.

TABLE II
TOLERANCE LIMITS OF CIRCUIT PARAMETER MISMATCH

Component	Tolerance
L	3%
C	3%
R	5%
μ	10%

C. Effects of Parameter Mismatch

So far, we have assumed identical parameter values for both the drive and response systems. In practice, parameter values in the two systems do vary, however small. It is therefore of interest to study of the effects of parameter mismatch on synchronization. This mismatch problem can be translated formally to the study of two slightly different systems [18]

$$\dot{\overline{x}} = f(\overline{x}(t), \mathbf{p}) \tag{22}$$

$$\dot{\overline{x}} = f(\overline{x}(t), \mathbf{p} + \delta\mathbf{p}) \tag{23}$$

where $\mathbf{p}$ is a vector of parameters, and $\delta\mathbf{p}$ is a vector of the differences in the values of $\mathbf{p}$ between the two systems. If we denote the variables for the response part of the two systems by $\overline{x}_R$ and $\overline{x}'_R$, similar to what has been discussed in Section II, then the condition for synchronization

Authorized licensed use limited to: Hong Kong Polytechnic University. Downloaded on December 18, 2008 at 21:24 from IEEE Xplore. Restrictions apply.

under a mismatch condition becomes $\lim_{t\to\infty} |\overline{x}'_R - \overline{x}_R| \leq \epsilon$ where ϵ is a vector of small numbers ($\epsilon_i \ll 1$ for all $i = 1, 2, \cdots, n$).

In this paper, instead of a formal mathematical study as outlined above, we examine the limits of parameter mismatch by computer simulations. Specifically, we keep the circuit parameters of the drive system unchanged and vary those of the response system one at a time. Table II shows the limits of parameter mismatch beyond which synchronization cannot be maintained. Both exact computer simulations and PSPICE simulations report the same findings.

VI. Conclusion

Power electronics circuits, due to their switching nonlinearity, exhibit a wide range of nonlinear and chaotic behavior. In recent years some results concerning bifurcations and chaos have been reported in power electronics systems and more are yet to be uncovered. In the nonlinear system literature, recent evidence of potential application in communication has aroused tremendous interest in chaos synchronization and dynamics of coupled systems. In this paper we consider, for the first time, power electronics circuits under a chaos synchronization context. We have shown in a simple drive-response connected system of chaotic power converters the possibility of synchronization. While any potential use of chaotic power converters remains uncertain, the present study provides a first evidence of synchronizing chaotic power converters. If power converters, apart from their normal power supply function, could be used to transmit messages, then future distributed power systems may serve the dual function of a power supply system and a medium of communication.

References

[1] L. M. Pecora and T. L. Carroll, "Synchronization in chaotic systems," *Phys. Rev. Lett.*, vol. 64, pp. 821–824, Feb. 1990.

[2] ——, "Driving systems with chaotic signals," *Phys. Rev. A*, vol. 44, pp. 2374–2383, Aug. 1991.

[3] L. Kocarev, K. S. Halle, K. Eckert, L. O. Chua, and U. Parlitz, "Experimental demonstration of secure communications via chaotic synchronization," *Int. J. Bifur. Chaos.*, vol. 2, no. 3, pp. 709–713, 1992.

[4] K. S. Halle, C. W. Wu, M. Itoh, and L. O. Chua, "Spread spectrum communication through modulatio of chaos," *Int. J. Bifur. Chaos*, vol. 3, no. 2, pp. 469–477, 1993.

[5] C. W. Wu and L. O. Chua, "A simple way to synchronize chaotic systems with applications to secure communication systems," *Int. J. Bifur. Chaos*, vol. 3, no. 6, pp. 1619–1627, 1993.

[6] H. Dedieu, M. P. Kennedy, and M. Hasler, "Chaos shift keying: Modulation and demodulation of a chaotic carrier using self-synchronizing Chua's circuit," *IEEE Trans. Circuits Syst. II*, vol. 40, pp. 634–642, Oct. 1993.

[7] U. Parlitz and L. Kocarev, "Multichannel communication using autosynchronization," *Int. J. Bifur. Chaos*, vol. 6, no. 3, pp. 581–588, 1996.

[8] D. C. Hamill, J. H. B. Deane, and J. Jefferies, "Modeling of chaotic dc-dc converters by iterated nonlinear mappings," *IEEE Trans. Power Electron.*, vol. 7, pp. 25–36, Jan. 1992.

[9] C. K. Tse, "Flip bifurcation and chaos in three-state boost switching regulators," *IEEE Trans. Circuits Syst. I*, vol. 41, pp. 16–23, Jan. 1994.

[10] E. Fossas and G. Olivar, "Study of chaos in the buck converter," *IEEE Trans. Circuits Syst. I*, vol. 43, pp. 13–25, Jan. 1996.

[11] S. Jalali, I. Dobson, R. H. Lasseter, and G. Venkataramanan, "Switching time bifurcations in a thyristor controlled reactor," *IEEE Trans. Circuits Syst. I*, vol. 43, pp. 209–218, Mar. 1996.

[12] M. di Bernardo, L. Glielmo, F. Garofalo, and F. Vasca, "Switching, bifurcations and chaos in dc/dc converters," *IEEE Trans. Circuits Syst. I*, vol. 45, pp. 133–141, Feb. 1998.

[13] S. Banerjee and K. Chakrabarty, "Nonlinear modeling and bifurcations in the boost converter," *IEEE Trans. Power Electron.*, vol. 13, pp. 252–260, Apr. 1998.

[14] S. C. Wong and Y. S. Lee, "SPICE modeling and simulation of hysteretic current-controlled Ćuk converter," *IEEE Trans. Power Electron.*, vol. 8, pp. 580–587, Oct. 1993.

[15] C. K. Tse, Y. M. Lai, and H. H. C. Iu, "Hopf bifurcation and chaos in a free-running current-controlled Ćuk switching regulator," *IEEE Trans. Circuits Syst. I*, vol. 47, pp. 448–457, Apr. 2000.

[16] R. D. Middlebrook and S. Ćuk, "A general unified approach to modeling switching power converter stages," *IEEE Power Electron. Specialists Conf. Rec.*, pp. 18–34, 1976.

[17] T. S. Parker and L. O. Chua, *Practical Numerical Algorithms for Chaotic Systems*. New York: Springer-Verlag, 1989.

[18] T. Kapitaniak, *Controlling Chaos*. London, U.K.: Academic, 1996.

Novel CMOS Current Feedback Op-Amp Realization Suitable for High Frequency Applications

Aly M. Ismail and Ahmed M. Soliman

***Abstract*—A novel CMOS current feedback operational amplifier (CFOA) is developed for wideband current-mode signal processing. The circuit has a very low input impedance over an exceptionally wide bandwidth and realizes an exact voltage-following action. Simulation results assuming 0.5-μm CMOS process shows that the impedance at the current input node is about 2 Ω and current and voltage transfer characteristics are extending beyond 180 MHz.**

***Index Terms*—CMOS circuits, current-feedback op amps.**

I. Introduction

In recent years, great interest has been devoted to the analysis and design of current-feedback and current-conveyor integrated circuits [1]–[9], mainly because these circuits exhibit better performance, particularly higher speed and better bandwidth, than classic voltage-mode operational amplifiers, which are limited by a constant gain-bandwidth product. The current-feedback operational amplifier (CFOA) is a four-port network with a describing matrix of the form

$$\begin{bmatrix} I_Y \\ V_X \\ I_Z \\ V_O \end{bmatrix} = \begin{bmatrix} 0 & 0 & 0 & 0 \\ 1 & 0 & 0 & 0 \\ 0 & 1 & 0 & 0 \\ 0 & 0 & 1 & 0 \end{bmatrix} \begin{bmatrix} V_Y \\ I_X \\ V_Z \\ I_O \end{bmatrix} \tag{1}$$

Several CMOS realizations for the CFOA have been reported in the literature [1]–[4]. The CFOA has been always seen as an extension of the CCII, therefore, the design approach was to cascade a CCII+ with a voltage follower to realize the complete circuit [3]. The obtained bandwidth was always a degraded version of the CCII+ bandwidth. A very interesting analysis for CFOA stability in high-frequency application was given in [2] where the basic structure of the CFOA implemented in bipolar technology and shown in Fig. 1 is considered. It has been shown that the stability of the CFOA can be ensured by considering the two dominant poles due to the equivalent impedance at the node Z and due to the current mirror conveying the current from the node X to the node Z. Typically, the current mirror pole frequency is much higher than the pole frequency due to the transimpedance pole of the amplifier. However, because of economic constraints, the

Manuscript received April 14, 1999; revised October 8, 1999. This paper was recommended by Associate Editor M. Biey.

The authors are with the Electronics and Communication Engineering Department, Cairo University, Giza, Egypt (e-mail: asoliman@idsc1.gov.eg).

Publisher Item Identifier S 1057-7122(00)05037-6.

1057–7122/00$10.00 © 2000 IEEE

Authorized licensed use limited to: Hong Kong Polytechnic University. Downloaded on December 18, 2008 at 21:24 from IEEE Xplore. Restrictions apply.